water

MDPI

Article

A Flood Inundation and Modelling Approach for Urban and Rural Areas in Ungauged Lake and Large-Scale River Basins

George Papaioannou [1,2,3,*], Lampros Vasiliades [2], Athanasios Loukas [4,*], Angelos Alamanos [5], Andreas Efstratiadis [6], Antonios Koukouvinos [6], Ioannis Tsoukalas [6] and Panayiotis Kossieris [6]

[1] Institute of Marine Biological Resources and Inland Waters, Hellenic Centre for Marine Research, 19013 Anavissos, Attiki, Greece
[2] Department of Civil Engineering, School of Engineering, University of Thessaly, 38334 Volos, Greece, lvassil@civ.uth.gr
[3] Studies program of the Department of Forestry and Natural Resources Management, General Department (Larisa), University of Thessaly, 43100 Karditsa, Greece
[4] School of Rural and Surveying Engineering, Aristotle University of Thessaloniki, 54124 Thessaloniki, Greece
[5] The Water Forum | Centre for Freshwater and Environmental Studies. Dundalk Institute of Technology, Marshes Upper, Dundalk Co. Louth, A91K584, Ireland, angelos.alamanos@dkit.ie
[6] Department of Water Resources and Environmental Engineering, School of Civil Engineering, National Technical University of Athens, 15780 Athens, Greece; andreas@itia.ntua.gr (A.E.); A.Koukouvinos@itia.ntua.gr (A.K.); jtsoukalas@hotmail.com (I.T.); pkossier@itia.ntua.gr (P.K.)
* Correspondence: gpapaioan@hcmr.gr (G.P.); agloukas@topo.auth.gr (A.L.) Tel.: +30-22910-76349 (G.P.); Tel: +30-2310996103 (A.L.)

Abstract: Fluvial floods are one of the primary natural hazards to our society, and the associated flood risk should always be evaluated for present and future conditions. The European Union's Floods Directive highlights the importance of flood mapping as a key-stage for detecting vulnerable areas, assessing floods' impacts, and identifying damages and compensation plans. The implementation of the E.U. Flood Directive in Greece is challenging, because of its geophysical and climatic variability and diverse hydrologic and hydraulic conditions. This study addresses this challenge by modelling of design rainfall at sub-watershed level and subsequent estimation of flood design hydrographs using the NRCS Unit Hydrograph Procedure. HEC-RAS 2D model is used for flood routing, estimation of flood attributes (i.e., water depths and flow velocities) and mapping of inundated areas. The modelling approach has been applied at two complex and ungauged representative basins: Lake Pamvotida basin located in the Epirus Region of the wet western Greece and Pinios River basin located in Thessaly Region of the drier central Greece, a basin with a complex dendritic hydrographic system, expanding to more than 1188 river-km. The proposed modelling approach aims to better estimation and mapping of flood inundation areas including relative uncertainties and providing guidance to professionals and academics.

Keywords: : EU Floods Directive; flood risk management; extreme rainfall; SCS-CN; 2D hydraulic modelling; HEC-RAS; fluvial floods; ungauged rivers

Citation: Lastname, F.; Lastname, F.; Lastname, F. Title. *Water* **2021**, *13*, x. https://doi.org/10.3390/xxxxx

Academic Editor: Firstname Lastname
Received: 04 March 2021
Accepted: date
Published: date

1. Introduction

Natural disasters caused by floods are responsible for the most casualties and economic loss in Europe and worldwide [1,2]. For example, for the period 1995–2015 floods affected 2.3 billion people and costed 157,000 human lives [3]. In general, there are five distinct types of floods (i.e. flash, fluvial, pluvial, urban and coastal floods), which may stem from various processes and sources. Flood impacts could be aggravated by human activities and interventions in the natural systems (e.g., deforestation, earthworks, water works, urbanisation). Fluvial (river) flooding is the most common type of flood and has global implications in our society since 50% of the world's population is close to freshwater bodies [4].

Flood hazard mapping is the process to address flood risk using a combination of structural and non-structural flood risk mitigation measures [5]. According to the EU Directive on floods (E.C. 2007/60), flood inundation mapping and risk assessment should be analyzed through appropriate and effective tools. Such techniques and methods are presented and discussed in recent review studies [6,7]. Usually, flood hazard mapping encompasses the determination of flood extent from synthetic flood events with typical design return periods (e.g., the 50-year return period flood). However, for accurate flood hazard mapping several other flood characteristics (i.e. flood depth, flow velocity, and rate of rising of the water) should be evaluated [6]. In engineering applications, flood extent and depth are the most common flood characteristics used: flood extent, because it allows for mapping flood events with typical return periods in a single map, and flooding depth, because it is directly associated with flood damage [8–10]. Both variables have been mainly assessed using one-dimensional (1D) hydraulic models [11,12]. However, the 1D-modelling method could lead to inaccurate findings under complex flow patterns and in low relief plain and urban areas. Hence, the use of 2D hydraulic modelling approaches is usually advocated for accurate flood hazard mapping [13–18].

Greece faces increasingly intense and frequent flood events over the last decades, thus their accurate modelling and mapping is becoming more and more important [19,20]. The areas that suffer particularly can be classified into three main categories [21]: i) closed hydrological basins, normally drained by natural sinkholes with limited drainage capacity, ii) plains traversed by complex river systems, and iii) urban areas, mainly affected by flash floods, where floodplains threat both wealth and human life. The presence of such catchments, at varying scales, combined with Greece's uneven rainfall distribution (wet conditions in the western part of the country and dry conditions in the central and eastern parts), creates a variety of cases that are difficult to be framed under a single hydraulic modelling approach. Subsequently, the implementation of the E.U. Flood Directive in Greece is challenging in terms of modelling and mapping, and becomes more challenging when considering the inherent uncertainties of hydrological and hydraulic simulations and the limitations in hydro-meteorological and flow data.

The above considerations are more general and they are among the most popular research questions in the field of flood inundation modelling and mapping [22,23]. Applying hydraulic modelling for flood inundation at large scale has been addressed by few researchers through coupled hydrologic and hydraulic models [24–29]. Previous relevant works on large-scale flood inundation modelling and mapping failed to address some important questions such as: 1) How one can manage a complex river system in which several sub-watersheds outflow to the central stem of a river? 2) How one can deal with a complex river system in which each sub-watershed outflow to a lake and the water of the lake outflow recharges another channel or stream? 3) Is it possible to provide better hydraulic geometry using finer resolution and incorporate several hydraulic structures within the geometry? Additionally, the most common sources of uncertainty are present at each stage of the modelling process, and are associated with: water input – rainfall (statistical uncertainty of design storms), the systems' initial conditions (hydrologic and runoff uncertainty, soil moisture conditions, etc.), and routing (roughness coefficient is a typical input and an uncertainty source in the hydraulic modelling) [30,31]. Despite the importance of these questions and modelling issues for the implementation of the E.U. Floods Directive in Greece, there aren't any studies, to the best of our knowledge, providing a framework for modelling large-scale basins with complex hydrographic network and closed basins forming lakes, including rural and urban areas.

This study aims to address important aspects of the above research questions through a new methodological framework for flood inundation modelling and mapping under uncertainty the follows the E.U. Flood Directive's requirements. The proposed framework is applied to two Greek basins with different features: a) the closed basin of

Lake Pamvotida located in Western Greece, and b) Pinios River located in Central Greece, draining a large-scale basin with a complex dendritic hydrographic system, expanding to more than 1188 river-km. The stages of the methodology include extreme precipitation modelling at sub-basin level, using spatially-distributed Intensity-Duration-Frequency (IDF) relationships, estimation of design hydrographs using the HEC-HMS model, where all time parameters are related to the rainfall intensity, flood routing and estimation of water depths and velocities by using the HEC-RAS 2D model, with flexible mesh size for urban areas, and mapping of inundated urban and rural areas of the study basins. Statistical, hydrological and hydraulic uncertainty factors are assessed by means of scenarios that refer to the parameters of IDF relationships, soil moisture conditions, and roughness coefficients, respectively. It should be mentioned that only fluvial, surface flooding (i.e., lake and/or river overflows) were investigated. These overflows may occur during the rising stage of a flood hydrograph and/or flash floods at the tributaries and during the rising stage of the hydrograph in the main stem of the river and/or lake related to a widespread, sustained high rainfall and ruptures of natural impoundments (e.g. lakes, lagoons and beaver dams) or artificial impoundments (e.g. obstructed bridges, dams), improper functioning or rupture of hydraulic structures (e.g. weirs, impoundment dams, reservoirs, artificial levees). The proposed approach presents a general methodology to address the above issues providing a useful reference for flood modelling and mapping analyses and its application in the two study basins, considering the specific features and modelling challenges.

2. Study Areas

2.1. Lake Pamvotida Catchment

Lake Pamvotida is located in a closed basin covering an area of 340 km^2, placed in Epirus Region, Northwestern Greece (Figure 1A). Most of the basin's runoff flows through small streams and torrents into the lake and a smaller portion of the runoff is diverted to the adjacent Kalamas River basin (to the northwest). The City of Ioannina, which is located at the middle of the western bank of the lake (Figure 1A), is the administrative center and the largest city of the Epirus Region. Its population is, about, 112,500 inhabitants, according to the 2011 census.

The study area's hydro-lithological conditions have been derived from the Management plans of flood risks for river basins in Epirous Region (Special Secretariat for Water & Ministry of Environment and Energy (SSW-MEE), 2018) [32]. Lake Pamvotida basin is covered by high to very high permeable formations (45%), followed by medium to low permeability formations (38%), very low to zero permeability formations (9%), and low permeability formations (8%). The basin’s altitude ranges from 469-1808 m with average elevation of about 680 m. The land cover classification used in this study was based on CORINE land-cover data. The main land cover classes prevailing at Lake Pamvotida basin are forested and semi-natural areas (44%) and agricultural areas (42.5%), followed by artificial surfaces (6.5%), water bodies (6%) and wetlands (1%).

The climate is mild, generally warm and temperate with very rainy winters, and dry summers. The average annual temperature is 13.2 °C. The average annual precipitation is about 1080 mm, with 123.7 rainfall days/year. It is the wettest area of Greece [33,34]. Extreme weather conditions are the main cause of flooding at the study basin. In the Ioannina city and the small island of Lake Pamvotida, houses were damaged and roads were flooded due to Lake overflows on the 9/12/2014 and on 14/11/2017 events [35,36]. The flooding processes and flood mapping studies for the study area are very limited, to the best of our knowledge.

2.2. Pinios River Basin

Pinios River basin extends over an area of 9,664 km^2 and is located in central Greece, covering most of the area of Thessaly Water District (TWD) (Figure 1B). The length of the main stem and the tributaries of Pinios River is estimated to be more than 1188 km, while the main channel is, approximately, 196 km long. Larisa city is located at the middle of the main channel of Pinios River (Figure 1B). It is one of the largest cities of Greece, and the financial and administrative center and the largest city of Thessaly Region. Its population is about 284,500 inhabitants, according to the 2011 census.

The climate of the basin is typical Mediterranean. The average annual rainfall and reference evapotranspiration are approximately 700 mm and 1,400 mm, respectively. The mean annual streamflow at the river delta is approximately 80 m^3/s [37,38]. Thessaly is the largest continuous agricultural productive plain of the country, and at the same time the driest Water District of Greece, which experiences frequent droughts and extreme rainfall events causing severe floods [39,40] that disrupt its productivity [41,42].

The area's hydro-lithological conditions have been derived from the Management plans of flood risks for river basins in Thessaly region (Special Secretariat for Water & Ministry of Environment and Energy (SSW-MEE), 2018). Pinios River basin is covered by medium permeability formations (42%), followed by very low to zero permeability formations (23%), low permeability formations (19%), high to very high permeable formations (12%), and low permeability formations (4%). The central part of the basin is covered by a large fertile plain of an area of about 4,000 km^2. The major cultivated crops are cotton, winter wheat, maise and alfalfa. Pinios River basin altitude ranges from 0 m to 2,085 m, with average elevation of about 440 m. The land cover classification used in this study was based on CORINE land-cover data. The main land cover classes prevailing at Pinios River basin are the agricultural areas (50.8%) and the forested and semi-natural areas (45.9%), followed by artificial surfaces (2.7%), water bodies (0.5%) and wetlands (0.1%).

Pinios River basin is known from the antiquity by the geographer Stravon for its floods, when the first protection works were structured. Besides the construction of a complex system of drainage channels, stream-lining works and land reclamation projects, already by the end of the 19th to the early 20th century, several parts of the basin are still prone to flooding [38]. Today, the broader region is considered as the most vulnerable in Greece, since the potential flood zones cover the 31.2% of its area (i.e. 4,172 of the 13,377 km^2 of the TWD) [43]. Quite often, extended inundations occur over the floodplains, resulting to significant damages to the agricultural production, with characteristic examples the recent events of February 2018 and September 2020. The middle stem of Pinios River is one of the major flood prone areas extends over a length of 40 km, between the flow stations of Ali Efenti and downstream Amygdalia (Figure 1B, from J7 to I1 and on). This river reach is located 15 km upstream of Larissa city. Furthermore, Tempi valley, as well as other narrow passes along the main river watercourse are intensify flooding in the Thessaly plain. Deforestation and urbanisation play also an important role increasing the destructive power of floods with consequence severe soil erosion problems. Thus, the interest of this study is focused on the main watercourse of Pinios River. Minor causes of flooding could be attributed to the inadequate natural discharge capacity across large parts of the river, the improper design of hydrotechnical projects (i.e. inadequate height of some bridges that have been built across the river, the construction by farmers of "handy" barriers in the river channel for storage of irrigation water). Finally, the low terrain elevation of the drainage network increases the flood risk at the study area. Historical flood events have been recorded and archived by the Ministry of Agriculture, the Ministry of Environmental, Physical Planning and Public Works and the Public Power Corporation during the last thirty years. The area around many villages such as Farkadona, Vlochos, Piniada and Koutsochero close to the junction of the rivers Kalentzis (Figure 1B, J6), Enipeas (Figure 1B, J3), Farsaliotis (Figure 1B, J4), Sofaditis (Figure 1B, J5) and Pinios (Figure 1B, J7), just after the outlet of the sub-basin at Keramidi bridge, is of a high flood risk area. Most scholars so far have focused on the analysis of the past events characteristics and the flood monitoring, rather that the modelling and mapping of flood events in the entire basin [19,20,44].

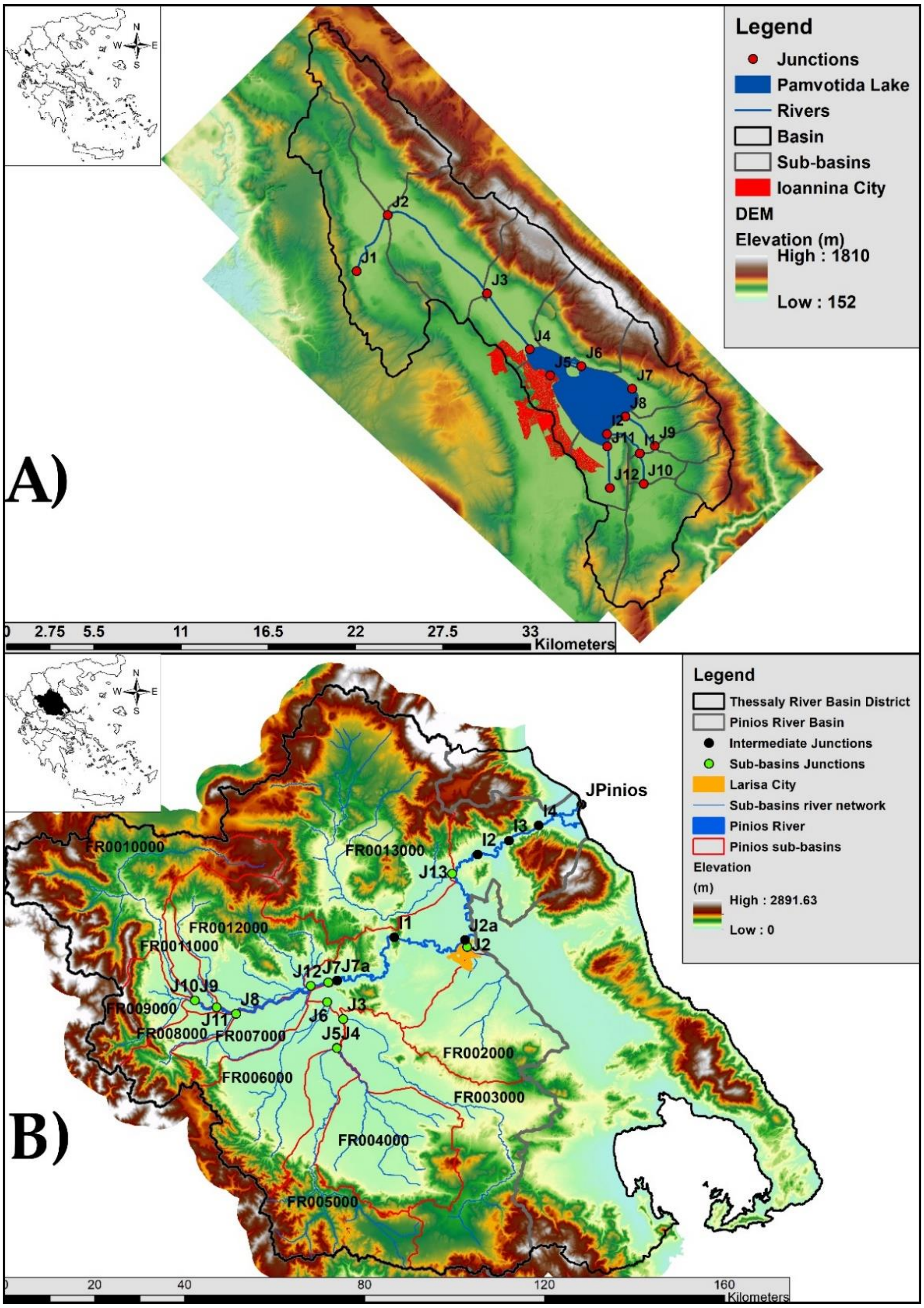

Figure 1. Study areas: (**A**) Pamvotida Lake basin and (**B**) Pinios River basin.

Both basins include rural areas, small settlements and two major cities, i.e. Ioannina city and Larisa city which are located on the bank of Pamvotida Lake and the main channel of Pinios River, respectively (Figures 1A, 1B). The above description makes clear the different features of the study areas and how challenging they are in terms of hydrologic and hydraulic modelling. The modelling approach presented in the following sections applies to both closed lake basins, and large-scale basins with complex and extended hydrographic network. In both cases, the urban areas are approached separately than the rural areas, in accordance with the E.U. Flood Directive.

3. Methodology

3.1. Flood Inundation Modelling and Mapping Approach

This study uses an integrated flood hazard and risk modelling and mapping framework developed for ungauged urban watersheds. The single event-based deterministic approach proposed by Papaioannou et al. [45] is adopted, comprising three modelling components: (i) synthetic storm generator; (ii) hydrological simulation model; and (iii) hydraulic simulation model. This is employed for three typical design return periods (T = 50, 100, 1000 years), assuming that the flood risk is connected to the determination of the input rainfall return period. The mathematical details can be found in the article of Papaioannou et al. [45], where emphasis is given on the hydrological analyses and the mathematical-theoretical background of hydraulic simulations. This paper focuses on the application of the framework to ungauged lake and large-scale complex river basins including urban, sub-urban and rural areas, which involve the hydraulic-hydrodynamic model's adaptation to specific conditions. Its successful implementation is expected to help water resource managers and decision makers to improve the design procedures for flood risk management of closed-lake basins and large-scale complex river basins, and may lead to more efficient flood mitigation strategies.

The hydraulic simulations are performed with a 2D modelling routine, to provide flood risk maps for T = 50, 100, 1000 years return periods, considering, an "average" and two "extreme" initial soil moisture hydrological scenarios. This approach allows for the estimation of lower and upper uncertainty bounds of the produced flood quantities, for each return period of interest. Overall, in the context of flood inundation and mapping, this approach can quantify the major sources of uncertainty: 1) statistical uncertainty associated with the parameters of IDF relationships (i.e., scale and location parameters), originating from limited samples of observed extreme rainfall data; 2) hydrologic uncertainty associated with the initial soil moisture conditions of the hydrological model, resulting to a wide range of the key input parameter of the SCS-CN method, i.e. the potential maximum retention; and 3) hydraulic–parametric uncertainty associated with Manning's roughness coefficient, which is a typical input parameter of hydraulic flow routing models. These three uncertainty components were combined, thus resulting to nine (9) operational scenarios (Table 1). The configuration of each scenario's assumptions is described in the next sections. Using the input hydrographs, the framework was run under these scenarios for each case study, considering, separately, the rural and the urban areas.

Table 1. Operational scenarios modelled to provide uncertainty bounds estimations.

Return Period	Hydrologic Conditions	Roughness Coefficient Conditions
T50	Dry (AMC_{I})	−50% Estimated
T50	Average (AMC_{II})	Estimated (Average)
T50	Wet (AMC_{III})	+50% Estimated
T100	Dry (AMC_{I})	−50% Estimated
T100	Average (AMC_{II})	Estimated (Average)
T100	Wet (AMC_{III})	+50% Estimated
T1000	Dry (AMC_{I})	−50% Estimated
T1000	Average (AMC_{II})	Estimated (Average)
T1000	Wet (AMC_{III})	+50% Estimated

3.2. Hydrological Modelling

This section presents the hydrologic modelling of the framework, comprising two parts, i.e. a storm generator and a rainfall-runoff model, providing the 'computational output (hydrographs) to be used as input to the hydraulic model. To account for the heterogeneity of the storm regime, a semi-distributed approach is followed, allowing to assign different rainfall inputs and model parameters across sub-basins and reach elements.

The procedure for extracting design hyetographs across sub-basins initiates with the estimation of partial rainfall depths for all temporal scales and return periods of interest, on the basis of spatially-averaged IDF relationships [46,47] for a standard design rainfall duration (D = 24 h). Design storm hyetographs are formulated with two typical time profiles, the Alternating Block Method, for T = 50 and 100 years, and the Worst Profile Method, for T = 1000 years [48–50]. These are next adjusted by using the areal reduction method, namely a dimensionless parameter that is defined as the ratio of areal to point rainfall, and is a decreasing function of the area and increasing function of duration) [51].

In order to account for joint statistical and hydrological uncertainties, three scenarios were formulated for each one of the three return periods (T = 50, 100, 1000 years), i.e., low, average and high. The design rainfall estimated by the IDF relationship is assumed to correspond to the average scenario, while its 80% confidence limits, which are measures of the statistical uncertainty induced by the estimation of IDF parameters from relatively small samples (i.e. annual maximum rainfall data), correspond to the two extreme scenarios (e.g. low-20% and high-80%) [52]. As mentioned in the previous section, hydrological uncertainty has been expressed in terms of the three typical Antecedent Moisture Conditions (AMC) that are accounted for in the SCS-CN approach [53]: dry (or low – AMC_{I}) represented by CNI, moderate (or average – AMC_{II}) represented by CNII, and wet (or high – AMC_{III}) represented by CNIII [45].

The transformation of the excess rainfall over each sub-basin to flood hydrograph at the outlet junction (rainfall-runoff model) is achieved using the dimensionless curvilinear unit hydrograph approach of SCS, which is considered the prevailing modeling approach for ungauged basins. Key assumption of the method was the implementation of the concept of varying (i.e., runoff-dependent) time of concentration, which affects the shape of unit hydrographs, thus introducing further nonlinearities to overall modelling approach [54]. The HEC-HMS software [55] was used, and the design flood hydrographs from the generated storms were estimated for all scenarios. Details are given in [45].

3.3. Hydraulic-Hydrodynamic Modelling

The Hydrologic Engineering Center (HEC) of United States Army Corps of Engineers developed the well-known HEC-RAS model that is used in many studies for 1D and 2D river flood modelling and floodplain management, e.g., [12,56]. The 2D hydrodynamic calculations are based on the 2D diffusive wave equations or the full 2D Saint-Venant equations [57]. A simplified version of the Navier-Stokes equations is the Shallow Water (SW) equations. The combination of the two-dimensional form of the Diffusion Wave Approximation and the mass conservation can yield the Diffusive Wave Approximation of the Shallow Water (DSW) equations. The two-dimensional (2D) HEC-RAS model is using the sub-grid bathymetry approach [57].

An important challenge in flood inundation modelling and mapping, especially for large-scale and complex watersheds, is the data requirement and preparation of the inputs into the hydraulic-hydrodynamic model [58]. The major requirements of the model are the Digital Elevation Model (DEM), the initial and boundary conditions (e.g., river flowpaths, banks, etc.), the roughness coefficients, the representation of technical works (e.g., hydraulic structures), and the representation of the urban areas by considering the effect of the building blocks to the water flow. The description of each component for the simulation of rural and urban areas is presented herein.

Several scholars [12,59–62] have highlighted the importance of the DEM accuracy in river flood modelling and mapping, especially in applications where a 2D hydraulic-hydrodynamic model is used. Recent developments in aerial photography regarding the improvements of spatial image resolution have led to high-resolution aerial photographs and orthophotos and by extension to sufficient DEM resolution for large scale river flood modelling and mapping at urban and rural areas [63]. In this study we use a DEM with resolution of 5 m, provided by National Cadastre and Mapping Agency S.A. (NCMA).

Roughness is a well-known input parameter in flood inundation modelling and mapping and a source of uncertainty. The selection of the appropriate methodology for a reasonable estimation of this parameter is an important step in flood inundation modelling and mapping [64,65]. The most common approach for large scale applications is the use of typical roughness coefficient values for various land uses, suggested in the international literature, combined with CORINE land cover data [38] for the floodplain roughness. Therefore, in this study typical Manning's roughness coefficient values were used in combination with CORINE land cover classification maps to estimate the average values of Manning's roughness coefficient over the floodplain (Figure 2). Haltas [66] studied the roughness coefficient calibration and showed that the use of a constant value for concrete surfaces, $n = 0.04$, can provide acceptable results. Therefore, a weighted roughness coefficient value has been used for small size urban areas such as villages ($n = 0.03$-0.04).

In flood inundation modelling, the channel roughness uncertainty prevails over the floodplain roughness uncertainty because the latter is estimated through a standard process [38,65,66]. Thus, in order to decrease the channel roughness uncertainty, the flood modelling expert estimated the average channel roughness values based on several photographs of the river, taken upstream and downstream of each technical river work, and riverine areas, aerial photographs examination (provided by NCMA) and typical Manning's roughness coefficient values that are proposed in the literature.

Another regulation of the E.U. Flood Directive implementation is the use of "upper" and "lower" boundaries of Manning's roughness coefficient. In this context, the average values of Figure 2 were adjusted by −50% and +50% to represent the upper and lower bounds of this parameter.

An important factor in river flood modelling, and especially, in 2D hydraulic hydrodynamic modelling, is the representation of technical works (e.g., flood protection works, culverts, bridges, weirs, etc.) within the river and the adjacent areas. In this study, the hydraulic structures were detected using aerial photographs, field observations, and data gathered from different local authorities. Next, accurate topographical surveys were conducted for the refining of important hydraulic structures [45]. All this information was used for the modification and/or correction of the DEM to depict accurately all-important hydraulic structures. In particular, the representation of bridges within the two-dimensional (2D) HEC-RAS model has been accomplished by employing a combination of weirs and culverts, modified in the RAS-Geometry routine.

Urban flood inundation modelling and mapping remain a challenge because of the multistage impact of flooding over these areas (social, economic, fatalities) and the complexity of the system. Recent studies focus on the building representation within the 2D hydraulic-hydrodynamic model for realistic simulation of flood inundation at urban areas [67–70]. The major building treatment methods are Building Resistance (BR), Building Block (BB), Building Hole (BH), and Building Parameter (BP) [70]. BR method involves the local rise of roughness coefficient value. BB and BH are similar, where in the BB method the building is represented using local rise of the elevation, while in BH the building blocks do not participate in the computational mesh of the hydraulic model. The BP method allows the water flowing within the block usually with the application of an area reduction factor (i.e. percentage of flooding participation in the building) [68,70]. Recent evidence [68,69] reveals the advantages and drawbacks of the building treatment methods and further work needs to be carried out to verify the optimum building treatment method. The Building Block (BB) approach was eventually used, in which the value of Manning's roughness coefficient for roads was set from 0.013 to 0.015.

Despite the technological advancements in 2D hydraulic modelling, flood inundation modeling using 2D approaches is still a time consuming and demanding task [63,71]. On the other hand, the model selection depends on the importance of the flooded areas (e.g. urban area, rural areas) and the output data requirements [71]. Thus, in cases where the use of a 2D hydraulic-hydrodynamic model is mandatory, the modeling process and its methodological steps can be a high-challenging issue. The following paragraphs present the design and implementation of specific methodological steps to overcome some of the 2D hydraulic modeling limitations.

The hydraulic-hydrodynamic modelling methodology developed for lakes and adjacent areas consists of the following steps: 1) hydrologic modelling of lake tributaries and estimation of flood flow inflow to the lake, 2) investigation and prioritization of hydraulic modelling domains (priority should be given to the tributaries that drain into the lake), 3) model configuration and preparation of model geometry for the examined tributaries, 4) river flood modeling, 5) preparation of the lake's hydraulic modelling geometry and hydraulic model configuration, where the lake state is put equal to maximum lake water level indicating the worst case scenario, 6) simulation of the lake as a closed system (since the lake receives the flow from all tributaries and the flow travels within the lake), 7) preparation of hydraulic modelling geometry outside of the lake and hydraulic model configuration, 8) simulation of flood inundation of rural and urban areas adjacent to the lake. The lake outflow estimated in step 6 is used as an inflow in this step. The lake works as tributary to the adjacent areas, 9) preparation of the hydraulic modelling geometry of the remaining areas and hydraulic model configuration, 10) simulation of flood inundation of the remaining areas. In case of areas connected in a row, the simulations should be implemented using a step-by-step possess, 11) all generated water depths are merged to a single file using max values to present the total inundation of the entire study area.

The hydraulic-hydrodynamic modelling methodology developed for large scale river flood modelling application consists of the following steps: 1) hydrologic modelling of river tributaries and estimation flood flow inflow to the river, 2) merging of flood hydrographs in junctions with common locations, 3) simulation of the first upstream river part, 4) re-estimation of flood flow inflow for the following river part. Before each simulation step should be undertaken adjustments, if needed, of the flow based on the participation of other tributaries that drain within the main channel 5) Simulation of flood inundation of following river part, 6) Repeat the steps 3,4,5 until the simulation of the river's final part. 7) Simulation of flood inundation of urban areas. It is applied only in cases that a city is located in the flooded area. The methodology for large-scale river flood modeling is an iterative step-by-step process and slowly shifts downstream. In cases where 2D simulation is not mandatory, or there is a gap between two 2D hydraulic domains, 1D simulation may be used for routing the flood wave in the following area. Finally, all generated water depths are merged to a single file using max values to depict the total inundation of the entire study area. The use of the step-by-step process overcomes the prohibited and problematic configuration and simulation of extremely large areas, however, it can be time consuming.

The hydraulic-hydrodynamic modelling methodology of urban areas follows similar steps with the already presented methodological steps. The main difference is in the preparation of the hydraulic modelling geometry where the terrain is modified based on the building blocks. Moreover, a finer mesh within the hydraulic modelling geometry should be used to accurately represent the complex urban terrain [45].

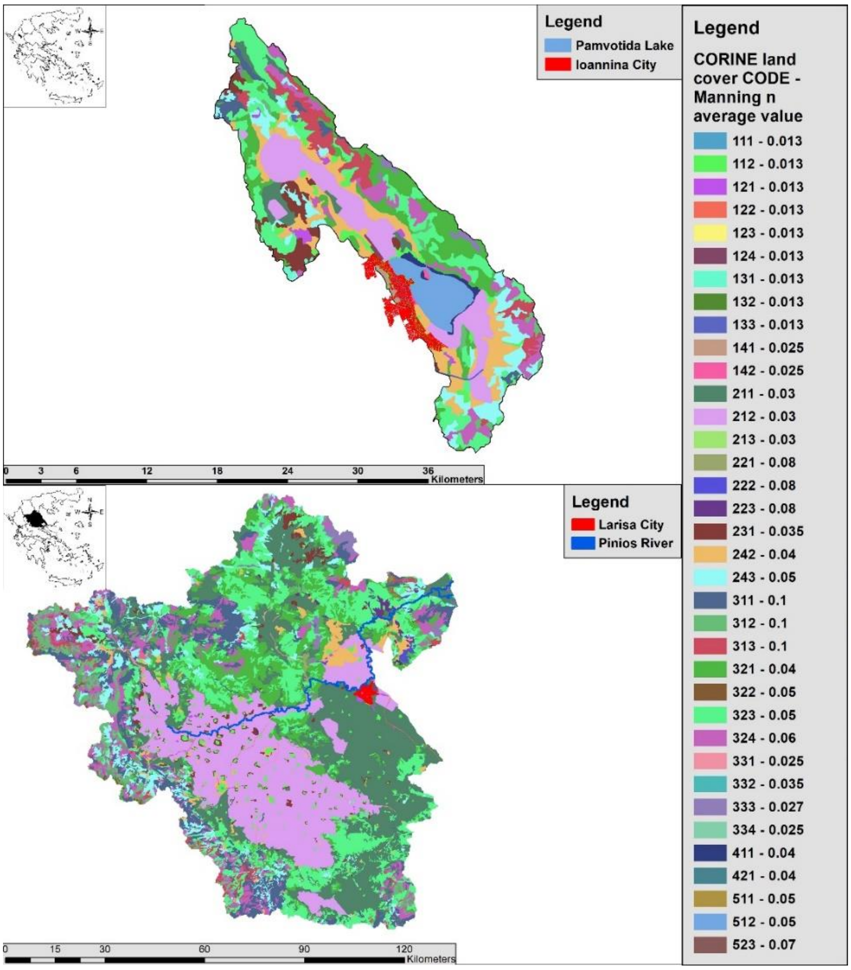

Figure 2. Average values of Manning's roughness coefficient based on CORINE land cover data for Pamvotida Lake (top map) and Pinios River (bottom map) basins.

3.4. Application of the modelling methodology to the study basins.

In this section, the specific adjustments of the general methodological framework and its application to the two study areas are described, as a reference point and guidance to future studies on similar areas. The main idea argues in favor of flexible modelling, as the only way to cope with the specific features of each given area. Thus, these adjustments refer to each stage of the process: hydrological, hydraulic-hydrodynamic, and of course the differences of rural and urban parts.

The two types of examined cases with the accompanying modelling challenges are:

- Closed basins–lakes; In the case of Pamvotida Lake (and every closed basin forming a lake) where there is not a hydrographic network that ends to a junction (i.e. basin’s outlet), the standard procedure for river network systems needs to be adapted. As explained below, the “exit” point (outlet) was simulated with a ‘virtual’ junction in the center of the lake.
- Large-scale basins with complex and extended hydrographic network (e.g. Pinios River), unavoidably are accompanied by huge computational load and required computational power, and need time-consuming processing. To tackle these impediments, a two-stage approach is followed, involving analytical modelling for each main tributary, and use of the associated outflow hydrographs as inputs for the hydraulic simulation of the main river (step-by-step approach).

With respect to the application of the hydrological modelling, the procedure described in section 3.2 was carried out. The sole difference between the two study areas was at the stage of the design hyetographs, i.e., the transformation of point to areal estimations. It must be noted that the rainfall areal reduction factor, φ, was applied in all examined cases (Pamvotida and Pinios River basins and sub-basins). Detail information about the application of the methodology is presented next for the two study basins.

Concerning the hydraulic modelling application, it is noteworthy to mention that the Flood Directive (2007/60/EC) implementation in Greece has been accomplished with the Flood Risk Management Plans (FRMP) and several methodological steps were implemented before the first version of the Greek FRMP. The first step was to undertake Preliminary Flood Risk Assessments (PFRA) leading to the identification of areas that are at significant risk of flooding, known as Areas of Potential Significant Flood Risk (APSFR) [72]. Consequently, Flood Hazard and Risk Maps (FHRM) were generated within the ASPFR in order to depict (e.g., water depth, velocity, flood extent) the impact of flooding that can affect human health, the economy, environment and cultural heritage [72,73]. Finally, FRMP were conducted using all previous results. Therefore, flood inundation modelling implemented only within the ASPFR areas.

3.4.1. Modelling of Pamvotida Lake system

Pamvotida Lake basin is a closed basin and the majority of the runoff from the sub-watersheds of the basin inflows into the lake and a small percentage of the basin runoff is diverted to the adjacent Kalamas River. The hydrological model domain consists of 15 sub-basins, 13 junctions, and 11 stream reaches, while the hydraulic-hydrodynamic model domain consists of eight (8) stream reaches (total length 47 km) and the lake (Figure 1A).

The hydraulic-hydrodynamic model configuration is restricted to these 8 reaches because, according to the general national guidelines, the flood inundation modelling was applied only within the potential flood inundation areas indentified in the preliminary flood risk assessment study. Thus, these 8 reaches were used for the simulation and routing of flood hydrographs and the estimation of flood hazard.

The special feature of Pamvotida Lake hydraulic modelling implementation is the division into two sub-domains: the inflow, and the outflow sub-domain. The lake basin consists of two independent hydraulic sub-systems, the downstream (4 sub-basins) and the upstream (10 sub-basins) that drains into the lake. One hydraulic geometry modelling configuration (i.e., the simulation from the Lake to the adjacent areas) was adjusted for urban flood inundation modelling for the area of Ioannina city. Considering the lake as a separate system, the outflow from all tributaries were used as input discharge to simulate the lake. The simulation set up of the lake aims to route the flow through the lake and to provide the outflow at J4 point (Figure 1A). Specifically, the inflow sub-domain consists of the hydraulic-hydrodynamic simulation of the runoff that directly enters into the lake (five inflow nodes, J5, J6, J7, J8, J11), while the outflow sub-domain consists of the hydraulic-hydrodynamic simulation of the outflow from the lake to the adjacent areas (one node, J4, and several outflow boundary lines) (Figure 1A). The mechanism of the outflow sub-domain initiates when the lake is at bankfull stage. Thus, when the lake water surface rises up to the water stage set by the regulating sluice gate, then part of the stored volume overflows to the lower sub-system (from node J4 to node J1), and then it is diverted to Kalamas River Basin through a canal (Figure 1A). Sixteen (16) technical works (e.g., bridges, culverts) have been surveyed, included in the digital topographical domain (i.e. revised DEM) and their effects on the flow are simulated. The generated mesh details for all Pamvotida Lake's hydraulic modelling domains are presented in Table 2.

3.4.2. Modelling of Pinios River basin system

The hydrological and hydraulic model of Pinios River basin consists of 12 sub-basins, 12 junctions, and 13 stream reaches (total length of about 196 km) including the Pinios River main channel (Figure 1B). The sub-basin areas range from 94 km^2 to 1,902 km^2 and their total area is approximately 8,410 km^2. The runoff from the sub-basins is routed through a number of major tributaries to the main channel of Pinios River. The outlet of Pinios River basin is at the Pinios Delta where the river outflows to the sea. The upstream part of the basin consists of 10 sub-basins, covering about 70% of its total area (Figure 1B), while the downstream part consists of only two (2) sub-basins (Figure 1B). The modelling system comprises twelve (12) junctions and six (6) intermediate nodes that work as junction points for multiple flood hydrographs and/or as midpoints. The main channel is divided into thirteen main reaches that involved within ASPFR and were simulated using the two dimensional (2D) hydraulic-hydrodynamic model. However, separating certain reaches from the rest of its hydrographic network, to comply with the ASPFR rules, creates a modelling challenge regarding the accurate estimations of their initial flows. For that purpose, we simulated separately the reaches that are not included within ASPFR zones. We used the 1D hydraulic-hydrodynamic modelling for the upstream parts, and their results were next set as input inflows to the zones included within the ASPFR (downstream parts). More specifically, the (upstream) reaches between the nodes I3 to I4 and J13 to I2 were simulated using the 1D hydraulic-hydrodynamic modelling approach to calculate the inflow of the (downstream) following areas that are included within the ASPFR zones (reaches between the nodes I2-I3 and I4-JPinios) (Figure 1B). Hence, the methodological 'gap' of the preliminary studies is covered, ensuring more accurate flow estimations for the zones of interest.

The flood hydrographs from the large sub-basins that are drained to Pinios (Figure 1B) were synchronized based on the Muskingum method [74]. Thus, main channel does not receive the flood hydrographs arriving from its tributaries at the same time. Some sub-basins such as FR003000 (J3), FR004000 (J4), FR005000 (J5), FR006000 (J6) (Figure 1B), are not connected directly to the Pinios main channel. In such cases the routing of the flood hydrographs till the main channel using the 2D hydraulic-hydrodynamic model.

It is well-known that the construction of IDF curves and asociated input rainfall events refer to a point, thus reuqiring a proper transformation to account for the spatio-temporal variability of rainfall across a river basin. The latter is typically achieved by applying a reduction coefficient φ, called Areal Reduction Factor, to the storm depths that are constructed through the two methods described in section 3.2. In this context, at all individual sub-basins, as well as the entire Pinios river basin of 9664 km^2, we applied the empirical formula proposed by Koutsoyiannis and Xanthopoulos [51]:

$$\varphi = 1 - \frac{0.048A^{0.36-0.01\ln(A)}}{d^{0.35}} \quad (1)$$

where A is the drainage area (km^2) and d is the rainfall duration (h).

At this point, the two-step modelling procedure introduces an inconsistency, since the reduction employed to each sub-basin is not in agrement with the reduction needed for the entire model domain. In theory, this would require to build *a priori* an exteremelly complex hydrological-hydraulic model to represent the full area of interest, which is yet impossible, due to the lack of computational recourses. In order to overcome this limitation, we adopted a hybrid approach, to adjust the computed output hydropgrahs from all sub-basins *a posteriori*. In this context, a dimensionless reduction coefficient, λ, was assigned to each sub-basin, i, defined as the ratio of the individual coefficients φ_i to the global coefficient φ_{Pinios} for the entire Pinios river basin, i.e. $\lambda_i = \varphi_i / \varphi_{Pinios}$. This asumption is based on the following proofs: 1) the value of φ_i is always less than one because it is not realistic to assign the same maximum rainfall intensity over large-scale river basins, 2) the larger sub-basins have smaller areal reduction factor values, which implies mor important reduction in the flood hydrograph, 3) increase in rainfall duration is followed by increase in the areal reduction factor, which means smaller reduction in the flood hydrograph, 4) the factor depends to some degree on the return period and it seems that the rise in the return period leads to small reduction of the areal reduction factor, which means smaller reduction in the flood hydrograph.

Hence, the reduction coefficient has been estimated for all Pinios river subbasins (12 sub-basins) and all flood hydrographs multiplied by the corresponding λ (Sub-basins junctions, Figure 1B, i.e., junction J5 flood hydrograph). Then, the hydraulic simulations of the main channel of Pinios river performed based on the final reduced outflow flood hydrographs of the 12 sub-basins (Sub-basins, Figure 1B, i.e. FR004000, FR003000, etc.).

Moreover, in certain cases, the flood hydrographs were merged because the outlets of some sub-basins were too close or at even the same location, or where there are multiple inflow junctions (e.g., see J9 and J10, Figure 1B). Thus, the modelling procedure is divided in a step-by-step (reach by reach) prossedure where the outflows of certain sub-basins were used as the inflows to the downstream reach, and the simulated outflow hydrograph of a reach was used as inflow hydrograph in the following (downstream) stream reach simulation. Furthermore, some parts of the Pinios river were bisected due to several limitation factors such as the enormous computational time, huge number of mesh elements, overdemanding computational power (e.g., see the reaches between the nodes J7 to I1 and I1 to J2 in Figure 1B). These techniques were proved to be the optimum ways to confront the case study's complexity. Finally, 21 technical works (e.g., bridges, culverts, river training works) have been digitised and included in the hydraulic-hydrodynamic model domain. For instance, Figure 3 presents the ground survey of Bridge 224 at Drosero (approximately 850 meters downstream from J9 and J10) (Figures 3A and 3B) and how these ground survey data are incorporated into the 2D hydaulic model (Figures 3A and 3B) (Figure 3C presents the technical details of the bridge piers and abutments and Figure 3D shows the effect of bridge design in the final mesh generation). The generated mesh details for all Pinios river hydraulic modelling domains are presented in Table 2.

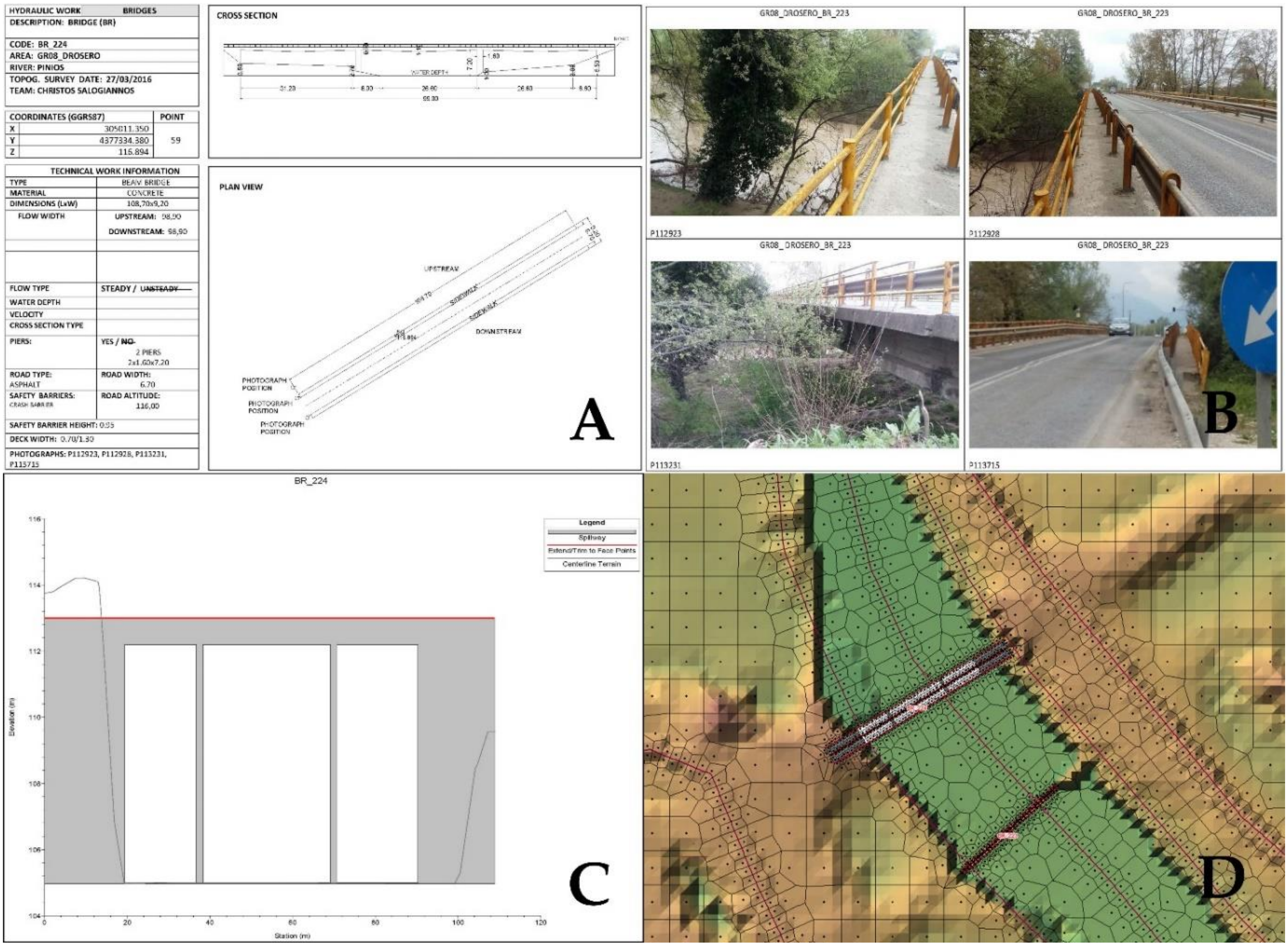

Figure 3. Example of ground survey of Bridge (Bridge number 224 at Drosero) (**A**) Topographical survey scketch., (**B**) Photographs from the topographical survey, (**C**) Technical details of the bridge piers and abutments, (**D**) Effect of bridge design in the final mesh generation.

Table 2. Generated mesh details for each junction at the two study watersheds.

Junctions	Min cell size (m²)	Average cell size (m²)	Max cell size (m²)	Number of Mesh cells
Pinios river basin				
I1 to J2	3.56	350.82	1,536.65	897,152
I4 to Jpinios	2.23	396.19	1,136.40	201,837
I2 to I3	3.15	170.52	355.7	136,643
J2 to J13	3.29	584.18	1,300.55	1,368,293
J3 to J6	11.1	461.99	1,320.13	380,244
J6 to J7a	9.75	434.43	912.19	298,897
J7a to I1	2.53	469.85	1,599	259,480
J7 to J7a	2.97	603.23	1,715.99	473,104
J8 to J12	2.83	619.13	1,337.19	1,402,636
J11 to J8	3.7	566.87	1,122.98	948,058
J12 to J7	17.99	605.26	1,145.23	448,332
J4J5 to J3	19.21	564.43	1252.93	630,411
J9J10 to J11	2.32	315.89	606.39	751,988
Lake Pamvotida basin				
Junctions	**Min cell size (m²)**	**Average cell size (m²)**	**Max cell size (m²)**	**Number of Mesh cells**
J12 to J11	7.39	179.65	879.34	45,238
I1 to I2	1.35	244.5	984.16	53,535
J10 to I1	4.47	325.88	726.51	19,547
J2 to J1	2.44	404.22	871.58	42,038

J3 to J2	2.3	403.84	1,064.81	82,064
J9 to J8	25.01	352.98	890.89	32,221
LAKE	355.53	628.6	1,643.88	35,345
LAKE OUT / J4 to J3	0.94	206.98	1,634.75	396,026

3.4.3. Hydraulic Modelling of Rural and Urban Areas

Flood inundation modelling and mapping were implemented using HEC-RAS 2D model with variable mesh computation point spacing, from 5 to 25 m. The diffusion wave equations were selected for all applications and a variable computational interval, from 1 to 10 s, has been used depended on the stability of each modelling application. The hydraulic-hydrodynamic modelling configurations consist of standard methods that followed at urban and rural areas applications. In most cases, the hydrograph output, the mapping output and the detailed output intervals were set to 15 minutes. The two categories of boundary conditions lines used are the inflow and the outflow ones. The former were defined by a hydrograph, while the latter were defined by normal depth [57,75].

The input DEM spatial resolution is 5 m, and a local increase of the elevation were implemented in the building block areas of Larisa city and Ioannina city (BB elevation rise method). In order to eliminate and/or correct the false representation of specific hydraulic structures and flood mitigation works, we used the actual topography of the structures and a DEM editing method that can generate a new surface using the geometry of cross sections (XS interpolation surfaces module of the RAS geometry routine) [76]. Several breaklines elements were used to provide different mesh resolution and an accurate representation of a) the river and its banks, b) the embankments and other flood mitigation works, c) the hydraulic structures (e.g. bridges, weirs, culverts, etc) and, d) the building block areas. For the Pinios River basin, two hydraulic geometry modelling configurations (i.e., see reaches between nodes I1 to J2, J2 to J13) were adjusted (i.e. BB elevation rise method) for urban flood inundation modelling of Larisa city.

3. Results and Discussion

The application of the semi-distributed hydrological modelling procedure was carried out for all the AMC scenarios, and the design hydrographs were produced from the HEC-HMS model. Figure 4 presents, indicatively, a set of inflow and outflow hydrographs estimated in junction J9-J10 (inflow) and junction J11 (outflow) of Pinios River for average AMC_{II}. Similarly, all the design hydrographs were estimated for each junction. The design hydrographs are then used as iputs to the hydraulic simulation for all examined hydrologic conditions, return periods and roughness coefficient scenarios.

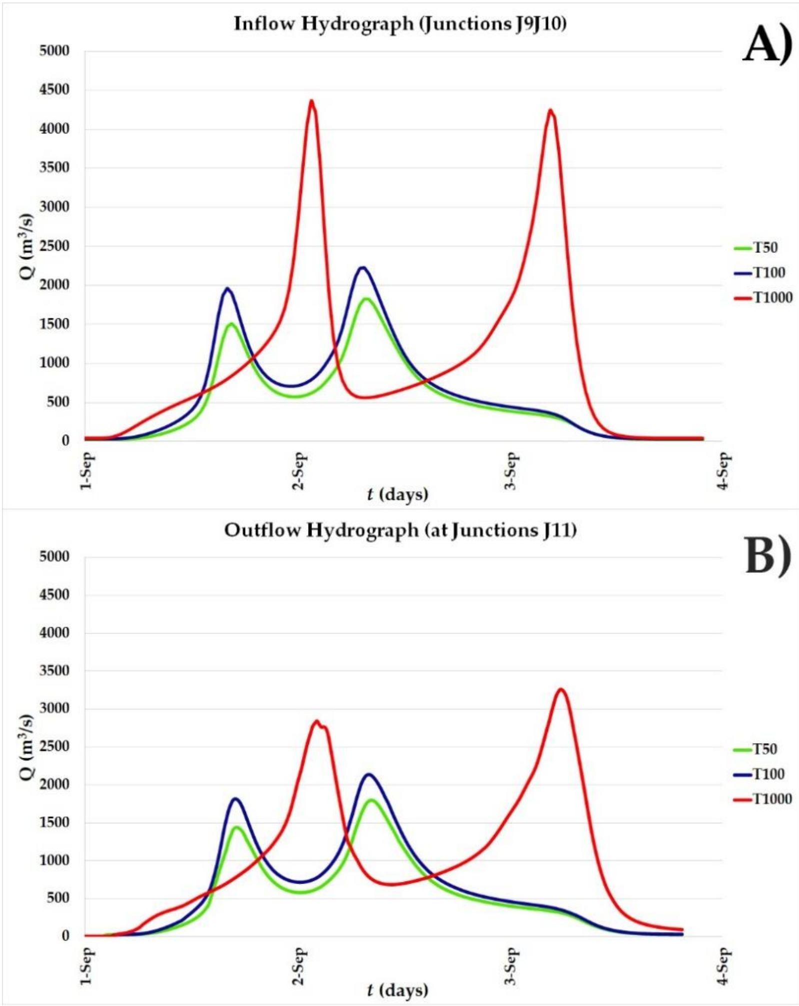

Figure 4. Inflow and outflow hydrographs estimated for junctions J9J10 and J11 respectively, of Pinios River for average AMCII for all return periods: (**A**) Inflow (design) hydrograph, (**B**) Outflow hydrograph.

The focus of this work is on the hydraulic simulation, which uses as inputs the produced hydrographs per junction. Table 3 presents Pamvotida Lake and Pinios River basins total flooded area (in km^2) for all examined scenarios and return periods, while a visual representation of Table 3 is presented in Figure 5 as Box and Whisker Plots. As expected, our results demonstrate that the flood inundation area is rising with the rise of the return period and with the change of the antecedent soil moisture conditions from dry to wet (Table 3, Figure 5).

It is interesting to note that based on the flooded area in the comparison of the hydrologic conditions the 3rd quartile 75% is wider than the 1st quartile, while in the comparison of the return periods the 1st quartile 25% is wider than the 3rd quartile. An important finding revealed from Table 3, and Figure 5 is that the effect of the hydrologic conditions' scenarios on the flood inundation area is more significant than the return period scenarios. The total flood inundation area of Pinios River varies from 157 to 463 km^2 for AMC_I, from 341 km^2 to 731 km^2 for AMC_{II}, and from 477 km^2 to 872 km^2 for AMC_{III}, while the flood inundation area of Lake Pamvotida ranges from 7.9 to 18.2 km^2 for AMC_I, from 16.3 to 26.7 km^2 for AMC_{II}, and from 19.6 to 34.0 km^2 for AMC_{III} (Table 3, Figure 5). This outcome confirms our previous findings [45], that the generation of a flood is strongly influenced by the soil moisture that is already stored at the beginning of rainfall.

A slight difference is observed between the flood inundation area of the operational scenarios for the return periods of 50 and 100 years, while a significant difference with the highest flood inundation area values is observed for the 1000-year return period (Table 3, Figure 5). The total flood inundation area of Pinios River varies from 157 to 477 km^2 for T=50 years, from 229 to 623 km^2 for T=100 years, and from 463 km^2 to 872 km^2 for T=1000 years, while the total flood inundation area of Lake Pamvotida ranges from 7.9 to 19.6 km^2 for T=50 years, from 11.5 to 24.4 km^2 for T=100 years, and from 18.2 to 34.0 km^2 for T=1000 years (Table 3, Figure 5).

Table 3. Lake Pamvotida and Pinios basin total flooded area (km^2) for all examined hydrologic and hydraulic scenarios and all investigated return periods.

Studies Basin	Hydrologic /Roughness Coefficient Scenarios	Return Period T (years)		
		50	100	1000
Lake Pamvotida	Dry (AMC_{I})/ −50%	7.89	11.47	18.17
	Average (AMC_{II})/ Average	16.34	20.06	26.69
	Wet (AMC_{III})/ +50%	19.56	24.42	34
Pinios River	Dry (AMC_{I})/ −50%	157	229	463.18
	Average (AMC_{II})/ Average	340.90	481.2	731.48
	Wet (AMC_{III})/ +50%	477	622.88	871.53

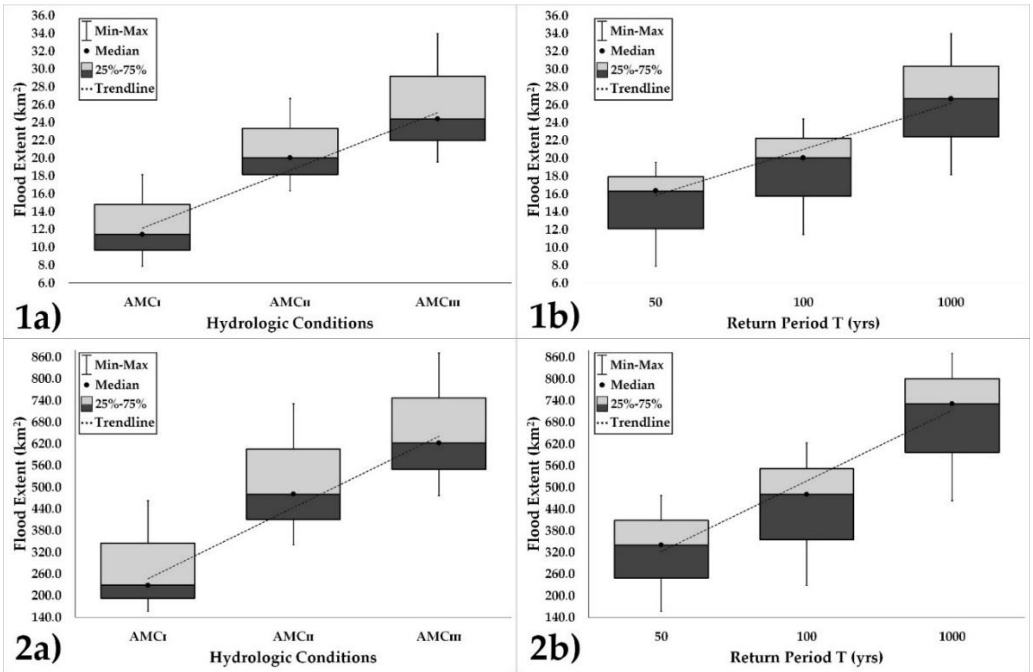

Figure 5. Box and Whisker plots based on the total flooded area (km^2) for all examined operational scenarios. The number of the figures denotes the case study [1) Pamvotida Lake, 2) Pinios River], while the letter of the figures denotes the hydrologic conditions [a)] and the return period [b)].

Figure 6 presents the maximum water depth and flood extent for all examined scenarios (all hydrologic conditions and return periods). The distribution of the maximum velocity for the average scenario for all return periods is presented in Figure 7. Figures 6 and 7 refer mainly to the rural parts of the study basins.

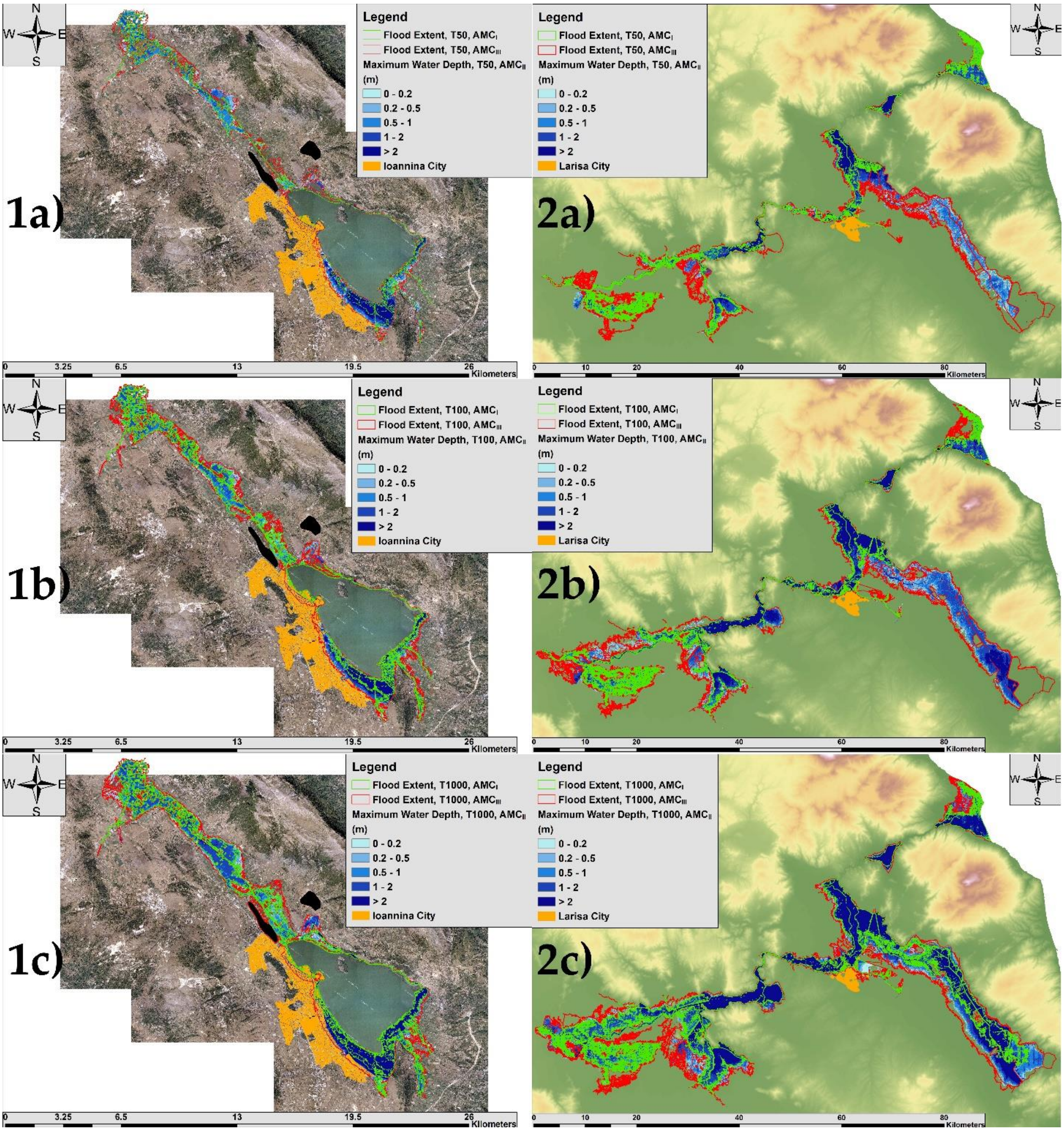

Figure 6. Maximum water depth and flood extent for all examined operational scenarios. The number of the figures denotes the case study [1) Pamvotida Lake, 2) Pinios river], while the letter of the figures denotes the return period [a) T = 50 years, b) T = 100 years, c) T = 1000 years].

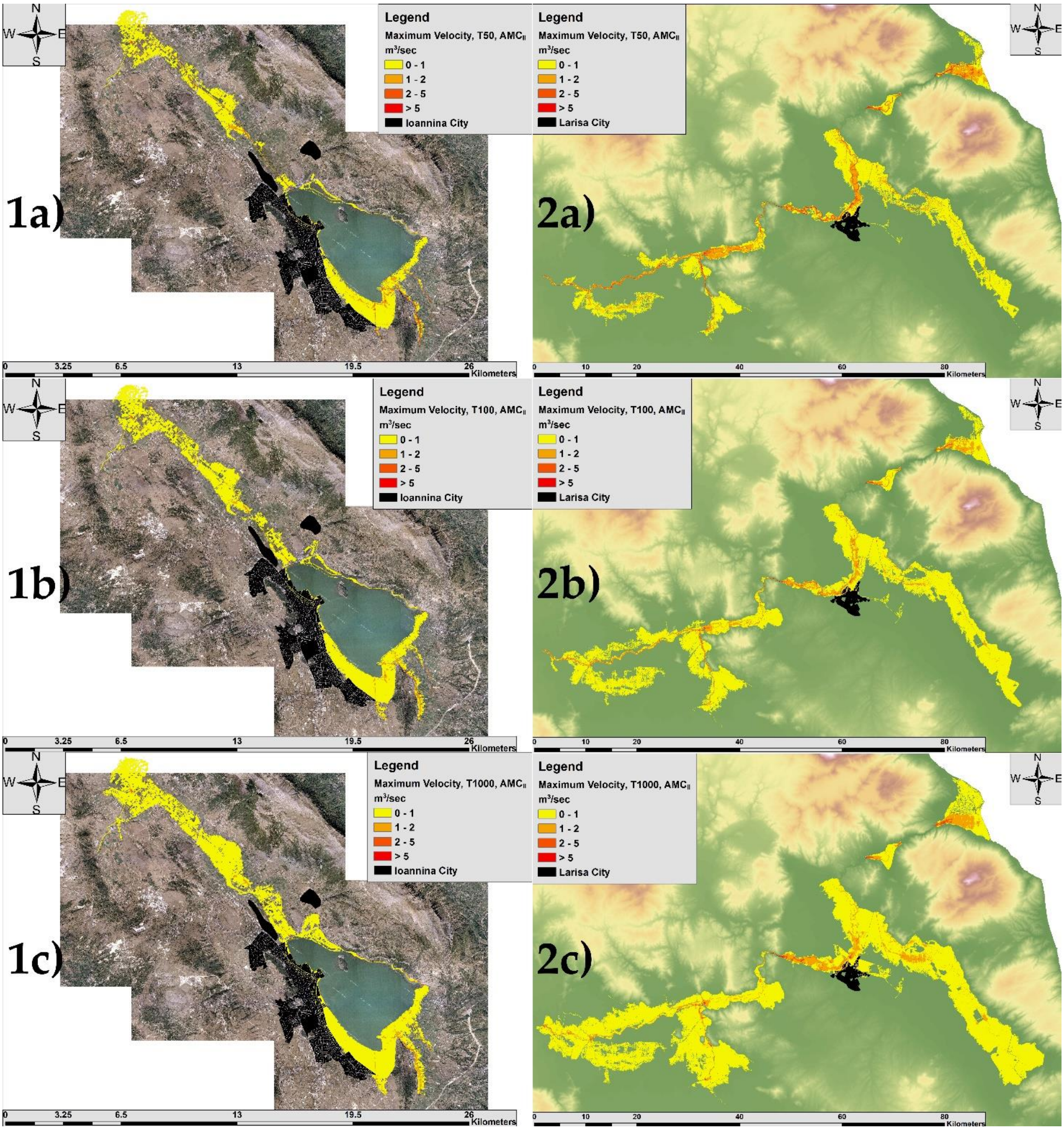

Figure 7. Maximum velocity for the average operational scenario. The number of the figures denotes the case study [1) Pamvotida Lake, 2) Pinios river], while the letter of the figures denotes the return period [a) T = 50 years, b) T = 100 years, c) T = 1000 years].

Since the simulations of urban areas need further attention, their results are presented in larger scale maps. Figure 8 presents the maximum water depth and the flood extent within the areas of Larisa and Ioannina cities for all scenarios and for the important return periods considered in urban areas (T = 50 years and T = 100 years). Interestingly, the water depth seems to be more sensitive than velocity (Figure 6, 7, 8). This is a reasonable finding, because of the terrain has small slope and thus, the flow velocities are low.

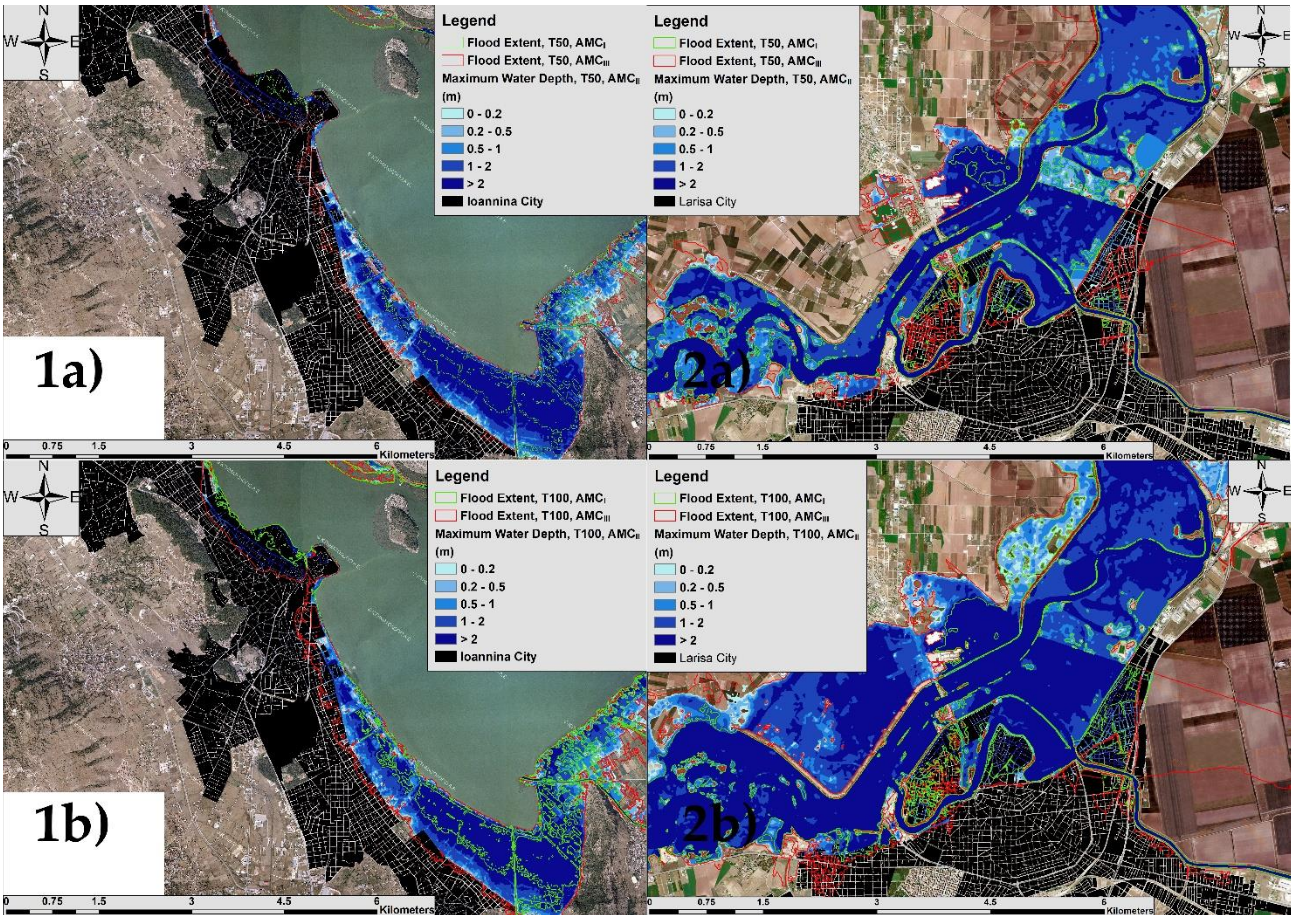

Figure 8. Maximum water depth and flood extent within the cities for all examined operational scenarios. The number of the figures denotes the case study [1) Pamvotida Lake-- City of Ioannina, 2) Pinios river- City of Larisa], while the letter of the figures denotes the return period [a) T = 50 year, b) T = 100 year].

The above results significantly vary due to the wide uncertainty bounds of the flood parameters (peak flows, flood volumes, inundated areas, etc.). The uncertainty bounds overlap the risk expressed by the return period of rainfall. Especially, the lower and upper estimations may differ by an order of magnitude for large return periods. For this reason, attention should be given in the application of the proposed methodology for specific return periods and hydrologic-hydraulic conditions. Finally, the findings of this study highlight the importance of using several scenarios (by means of hydrologic and hydraulic-hydrodynamic configurations) to quantify the associated uncertainty, to select the optimum configuration for flood inundation modelling and mapping and to use the results for the improvement of flood risk mitigation strategies.

5. Conclusions

This paper presents a hydrologic-hydraulic-hydrodynamic computational framework for flood modelling. All configurations concerning the flood modelling and mapping at urban and rural areas are in line with the E.U. Flood Directive. Each member-state has the versatility in determining the optimum configuration of the framework, customized to their context of flood management, aiming to accurate estimations and representations of potential risks [77].

A limitation regarding its application in Greece, is that the national datasets of flood records lack in detail, accuracy, and spatial distribution of the recorded flood characteristics (water depth, flood extent, rainfall, etc.), so typical approaches such as data-driven approaches in flood risk assessment, based on observed floods statistical analysis, are not feasible [20,78]. Typical hydrological and hydraulic methods and flexible modelling settings were counterposed. The input data uncertainties issue was further addressed by using scenario-based approaches (regarding extreme rainfall analysis, antecedent soil moisture conditions, and roughness coefficient). Such scenarios are recommended to estimate upper and lower water depth, velocities, and inundated areas for each return period, thus quantifying the uncertainties introduced by each parameter.

An advantage of this work is that the examples presented cover in general, the most flood-prone areas such as closed hydrological basins drained by natural sinkholes with limited drainage capacity, plains traversed by complex river systems, and urban areas. Motivated by the peculiarities of Greek areas in terms of hydraulic simulation, the different case studies were presented as examples to provide guidance on how to address several broader hydraulic-hydrodynamic modelling concerns. Although using more than one case study increases the working effort, it is recommended for testing a model (as a generally applicable design framework). The proposed approaches and the main hydraulic-hydrodynamic modelling configurations are generalized and summarized in Table 4. Their results provide all the necessary elements for flood management.

Table 4. Hydraulic-hydrodynamic configurations and techniques recommended for the modelling of rural and urban areas in closed lake basins and large-scale complex river basins.

Recommendations for each modelling category	**Description–Steps**
General: for rural and urban areas **Goal:** increase accuracy & facilitate computations	• Make necessary DEM modifications (e.g., at urban areas, building representation using local elevation rise BB method). • Roughness coefficient estimation using CORINE land cover, standard roughness coefficient tables, and refine with more detailed photos and relevant literature (in certain parts). • The technical works (bridges, culverts, embankments, etc.) were configured within the hydraulic-hydrodynamic geometry configuration. • Consider different case studies with different features to test the model as a framework.
Case 1: closed basins with limited drainage **Specific goal:** address areas that do not have an 'exit' point as outlet of the catchment (i.e., outlet is considered as a bankfull lake). Thus, such lake, can be examined on their water-expantion under the conditions imposed by the design storms.	1) Hydrologic modelling of lake tributaries and estimation flood flow inflows to the lake. 2) Flood inundation modelling of lake tributaries (general recommendations). 3) Two different simulation approaches (lake inflow and lake outflow simulations) were conducted for the lake system. ○ The lake was simulated as a closed system, as well as its outflows to the adjacent areas. The inflows were added from its outer boundaries, as the surplus of their normal flow conditions, while the outlet is considered to be a virtual junction in the centre of the lake. ○ Simulation of flood inundation of rural and urban areas adjacent to the lake (general recommendations).
Case 2: large-scale regions with complex hydrographic network **Specific Goal:** address huge computational requirements maintaining the desirable accuracy.	1) Hydrologic modelling of river tributaries and estimation flood flow inflow to the river. 2) Merging flood hydrographs in junctions with common locations (step-by-step procedure). 3) Simulate the river's upstream, then re-estimate flood inflows for the downstream. 4) Simulate flood inundation of following part of the river. 5) Simulate flood inundation of urban areas. 6) For large rivers, follow an iterative procedure, by repeating steps 3 and 4 till the simulation of the final part of the river.
Uncertainty **Goal:** improve the model, be aware of values' range, warn for uncertainty sources.	• Develop scenarios by detecting the most important sources of uncertainty (e.g., extreme rainfall estimations, antecedent soil moisture conditions, roughness coefficients). • Include them in the modelling procedure and examine the uncertainty bounds.

Although the limitation regarding large computational time for the large-scale areas remains, since it is a step-by-step procedure, it provides more accurate estimations. The successful implementation of the proposed framework is a valuable advance for the improvement of flood risk mitigation studies and indicate the uncertainty introduced in flood risk management in rural and urban areas using typical engineering practices.

The evidence from this study indicates that the input data uncertainty of the hydrologic analysis (e.g., antecedent soil moisture conditions and extreme rainfall estimations) may prevail against the probability of rainfall per se, which is expressed in terms of return period. Even though the studied input data uncertainty prevailed in the analysis, it is underlined that these parameters are not the only sources of uncertainty within the hydrologic analysis. Therefore, flood inundation modelling under additional uncertainty scenarios is suggested.

Actually, there are several other challenges can be encountered when performing hydraulic-hydrodynamic modelling. However, a key-message of this work is the flexibility of the techniques and methods that must accompany the mindset of the analyst when approaching challenging and compelling problems. This is in line with other recent modelling advances, not only referring to floods, and its importance is further highlighted when data limitations need to be addressed [79–81]. The combination of deep knowledge of the theoretical background (conceptually and mathematically) and the computational context (tools) is required, and comes through practice and experience.

Author Contributions: Conceptualization, methodology, formal analysis, writing—original draft preparation, visualisation, G.P., A.L., L.V. and A.E., writing—original draft preparation, visualisation A.A., formal analysis A.K., I.T. and P.K. All authors have read and agreed to the published version of the manuscript.

Funding: This research received no external funding

Data Availability Statement: The data that support the findings of this study are available from the Greek Ministry of Environment and Energy - Special Secretariat for Water (SSW). Specific data can be provided by the corresponding author upon reasonable request.

Acknowledgments: This paper is part of the project "Management Plans of Flood Risks for River Basins in Thessaly, Western Sterea Hellas and Epirus Regions, Greece", co-funded by the E.U. and the Greek Ministry of Energy and the Environment. This project constitutes the implementation of the EU Directive on Floods (E.C. 2007/60) in the above regions of Greece. The research presented in the paper is partially supported by this project.

Conflicts of Interest: The authors declare no conflict of interest.

References

1. Berz, G.; Kron, W.; Loster, T.; Rauch, E.; Schimetschek, J.; Schmieder, J.; Siebert, A.; Smolka, A.; Wirtz, A. World map of natural hazards - a global view of the distribution and intensity of significant exposures. *Nat. Hazards* **2001**, *23*, 443–465, doi:10.1023/A:1011193724026.
2. Barredo, J.I. Normalised flood losses in Europe: 1970-2006. *Nat. Hazards Earth Syst. Sci.* **2009**, *9*, 97–104, doi:10.5194/nhess-9-97-2009.
3. Wallemacq, P.; Guha-Sapir, D.; McClean, D.; CRED; UNISDR *The Human Cost of Weather Related Disasters - 1995 - 2015*; 2015;
4. Kummu, M.; de Moel, H.; Ward, P.J.; Varis, O. How close do we live to water? a global analysis of population distance to freshwater bodies. *PLoS One* **2011**, *6*, doi:10.1371/journal.pone.0020578.
5. Kreibich, H.; Bubeck, P.; Van Vliet, M.; De Moel, H. A review of damage-reducing measures to manage fluvial flood risks in a changing climate. *Mitig. Adapt. Strateg. Glob. Chang.* **2015**, *20*, 967–989, doi:10.1007/s11027-014-9629-5.
6. De Moel, H.; Van Alphen, J.; Aerts, J.C.J.H. Flood maps in Europe - Methods, availability and use. *Nat. Hazards Earth Syst. Sci.* **2009**, *9*, 289–301, doi:10.5194/nhess-9-289-2009.
7. Tsakiris, G. Flood risk assessment: Concepts, modelling, applications. *Nat. Hazards Earth Syst. Sci.* **2014**, *14*, 1361–1369, doi:10.5194/nhess-14-1361-2014.
8. Smith D Flood damage estimation A review of urban stage damage curves and loss functions. *Water SA* **1994**, *20*, 231–238.
9. Jongman, B.; Kreibich, H.; Apel, H.; Barredo, J.I.; Bates, P.D.; Feyen, L.; Gericke, A.; Neal, J.; Aerts, J.C.J.H.; Ward, P.J. Comparative flood damage model assessment: Towards a European approach. *Nat. Hazards Earth Syst. Sci.* **2012**, *12*, 3733–3752, doi:10.5194/nhess-12-3733-2012.

10. Huizinga, J.; Moel, H. de; Szewczyk, W. *Global flood depth-damage functions : Methodology and the Database with Guidelines*; 2017;
11. Aronica, G.; Bates, P.D.; Horritt, M.S. Assessing the uncertainty in distributed model predictions using observed binary pattern information within GLUE. *Hydrol. Process.* **2002**, *16*, 2001–2016, doi:10.1002/hyp.398.
12. Papaioannou, G.; Loukas, A.; Vasiliades, L.; Aronica, G.T. Flood inundation mapping sensitivity to riverine spatial resolution and modelling approach. *Nat. Hazards* **2016**, *83*, 117–132, doi:10.1007/s11069-016-2382-1.
13. Teng, J.; Jakeman, A.J.; Vaze, J.; Croke, B.F.W.; Dutta, D.; Kim, S. Flood inundation modelling: A review of methods, recent advances and uncertainty analysis. *Environ. Model. Softw.* **2017**, *90*, 201–216, doi:10.1016/j.envsoft.2017.01.006.
14. Horritt, M.S.; Bates, P.D. Evaluation of 1D and 2D numerical models for predicting river flood inundation. *J. Hydrol.* **2002**, *268*, 87–99, doi:10.1016/S0022-1694(02)00121-X.
15. Néelz, S.; Pender, G. *Desktop Review of 2D Hydraulic Modelling Packages. DEFRA/Environment Agency, UK.*; 2009;
16. Neelz, S.; Pender, G.; Wright, N.G. *Benchmarking of 2D Hydraulic Modelling Packages*; Bristol, 2010;
17. Neelz, S.; Pender, G. *Benchmarking the latest generation of 2D Hydraulic Modelling Packages*; 2013;
18. Papaioannou, G.; Vasiliades, L.; Loukas, A.; Aronica, G.T. Probabilistic flood inundation mapping at ungauged streams due to roughness coefficient uncertainty in hydraulic modelling. *Adv. Geosci.* **2017**, *44*, 23–34, doi:10.5194/adgeo-44-23-2017.
19. Bathrellos, G.D.; Skilodimou, H.D.; Soukis, K.; Koskeridou, E. Temporal and spatial analysis of flood occurrences in the drainage basin of Pinios River (Thessaly, Central Greece). *Land* **2018**, *7*, 1–18, doi:10.3390/land7030106.
20. Diakakis, M.; Mavroulis, S.; Deligiannakis, G. Floods in Greece, a statistical and spatial approach. *Nat. Hazards* **2012**, *62*, 485–500, doi:10.1007/s11069-012-0090-z.
21. Mimikou, M.; Koutsoyiannis, D. Extreme floods in Greece:The case of 1994. In Proceedings of the U.S. - ITALY Research Workshop on the Hydrometeorology, Impacts, and Management of Extreme Floods; 1995; pp. 13–17.
22. *Hydraulic Modeling: Concepts and Practice*; Ettema, R., Ed.; American Society of Civil Engineers, 2000; ISBN 978-0-7844-7041-1.
23. Nkwunonwo, U.C.; Whitworth, M.; Baily, B. A review of the current status of flood modelling for urban flood risk management in the developing countries. *Sci. African* **2020**, *7*, e00269, doi:10.1016/j.sciaf.2020.e00269.
24. Falter, D.; Dung, N. V.; Vorogushyn, S.; Schröter, K.; Hundecha, Y.; Kreibich, H.; Apel, H.; Theisselmann, F.; Merz, B. Continuous, large-scale simulation model for flood risk assessments: Proof-of-concept. *J. Flood Risk Manag.* **2016**, *9*, 3–21, doi:10.1111/jfr3.12105.
25. De Paiva, R.C.D.; Buarque, D.C.; Collischonn, W.; Bonnet, M.P.; Frappart, F.; Calmant, S.; Bulhões Mendes, C.A. Large-scale hydrologic and hydrodynamic modeling of the Amazon River basin. *Water Resour. Res.* **2013**, *49*, 1226–1243, doi:10.1002/wrcr.20067.
26. Neal, J.; Schumann, G.; Bates, P. A subgrid channel model for simulating river hydraulics and floodplain inundation over large and data sparse areas. *Water Resour. Res.* **2012**, *48*, 1–16, doi:10.1029/2012WR012514.
27. Biancamaria, S.; Bates, P.D.; Boone, A.; Mognard, N.M. Large-scale coupled hydrologic and hydraulic modelling of the Ob river in Siberia. *J. Hydrol.* **2009**, *379*, 136–150, doi:10.1016/j.jhydrol.2009.09.054.
28. Klimeš, J.; Benešová, M.; Vilímek, V.; Bouška, P.; Cochachin Rapre, A. The reconstruction of a glacial lake outburst flood using HEC-RAS and its significance for future hazard assessments: An example from Lake 513 in the Cordillera Blanca, Peru. *Nat. Hazards* **2014**, *71*, 1617–1638, doi:10.1007/s11069-013-0968-4.
29. Greenberg, R.J. DAM BREACH MODEL OF LAKE ANZA DAM USING HEC-RAS, California State University, Sacramento, 2018.
30. Pathak, C.S.; Teegavarapu, R.S. V.; Olson, C.; Singh, A.; Lal, A.M.W.; Polatel, C.; Zahraeifard, V.; Senarath, S.U.S. Uncertainty Analyses in Hydrologic/Hydraulic Modeling: Challenges and Proposed Resolutions. *J. Hydrol. Eng.* **2015**, *20*, 02515003, doi:10.1061/(ASCE)HE.1943-5584.0001231.
31. Annis, A.; Nardi, F.; Volpi, E.; Fiori, A. Quantifying the relative impact of hydrological and hydraulic modelling parameterizations on uncertainty of inundation maps. *Hydrol. Sci. J.* **2020**, *65*, 507–523, doi:10.1080/02626667.2019.1709640.
32. Special Secretariat for Water; Ministry of Environment and Energy (SSW-MEE) *Flood Risks for River Basins in Epirous Region. Analysis of area characteristics and flood mechanisms*; 2015;
33. WEATHER-ATLAS Available online: https://www.weather-atlas.com/en/greece/ioannina-weather-october (accessed on Jan 8, 2021).
34. CLIMATE-DATA.ORG Available online: https://en.climate-data.org/europe/greece/ioannina/ioannina-1375/ (accessed on Jan 8, 2021).
35. Zikakou, I. Flooding on Ioannina Lake Island Available online: https://greece.greekreporter.com/2014/12/09/flooding-on-ioannina-lake-island/ (accessed on Jun 12, 2020).
36. Davies, R. Greece – Floods in North West Leave 1 Dead Available online: http://floodlist.com/europe/greece-floods-corfu-epirus-november-2017 (accessed on Jun 12, 2020).
37. Vasiliades, L.; Loukas, A.; Liberis, N. A Water Balance Derived Drought Index for Pinios River Basin, Greece. *Water Resour. Manag.* **2011**, *25*, 1087–1101, doi:10.1007/s11269-010-9665-1.
38. Dimitriadis, P.; Tegos, A.; Oikonomou, A.; Pagana, V.; Koukouvinos, A.; Mamassis, N.; Koutsoyiannis, D.; Efstratiadis, A. Comparative evaluation of 1D and quasi-2D hydraulic models based on benchmark and real-world applications for uncertainty assessment in flood mapping. *J. Hydrol.* **2016**, *534*, 478–492, doi:10.1016/j.jhydrol.2016.01.020.
39. Loukas, A.; Vasiliades, L. Probabilistic analysis of drought spatiotemporal characteristics in Thessaly region, Greece. *Nat. Hazards Earth Syst. Sci.* **2004**, *4*, 719–731, doi:10.5194/nhess-4-719-2004.

40. Ameziane, T.; Belghiti, M.; Benbeniste, S.; Bergaoui, M.; Bonaccorso, B.; Cancelliere, A.; Christofides, T.; Cubillo, F.; Euchi, L.; Gabiña, D.; et al. *Drought Management Instructions*; 2007;
41. Davies, R. Greece – Evacuations After Floods in Thessaly Available online: http://floodlist.com/europe/greece-floods-thessaly-february-march-2018.
42. Copernicus - Mapping Emergency Management Service EMSR271: Floods in Central Greece Available online: https://emergency.copernicus.eu/mapping/list-of-components/EMSR271/ALL/ALL (accessed on Feb 1, 2019).
43. Special Secretariat for Water; Ministry of Environment and Energy (SSW-MEE) *Flood Risks for River Basins in Thessaly Region. Analysis of area characteristics and flood mechanisms.*; 2017;
44. Psomiadis, E.; Soulis, K.X.; Zoka, M.; Dercas, N. Synergistic approach of remote sensing and gis techniques for flash-flood monitoring and damage assessment in Thessaly plain area, Greece. *Water (Switzerland)* **2019**, *11*, doi:10.3390/w11030448.
45. Papaioannou, G.; Efstratiadis, A.; Vasiliades, L.; Loukas, A.; Papalexiou, S.; Koukouvinos, A.; Tsoukalas, I.; Kossieris, P. An Operational Method for Flood Directive Implementation in Ungauged Urban Areas. *Hydrology* **2018**, *5*, 24, doi:10.3390/hydrology5020024.
46. Efstratiadis, A.; Papalexiou, S.M.; Markonis, I.; Mamassis, N. *Management Plans of Flood Risks for River Basins in Epirous, Greece (GR08)–Phase A -Ombrian curves*; 2015;
47. Efstratiadis, A.; Papalexiou, S.M.; Markonis, I.; Mamassis, N. *Management Plans of Flood Risks for River Basins in Thessaly, Greece (GR08)–Phase A -Ombrian curves*; 2015;
48. Koutsoyiannis, D. A stochastic disaggregation method for design storm and flood synthesis. *J. Hydrol.* **1994**, *156*, 193–225, doi:10.1016/0022-1694(94)90078-7.
49. Sutcliffe, J. V *Methods of flood estimation: a guide to the Flood Studies Report*; Institute of Hydrology: Wallingford, 1978;
50. Chow, V.; Maidment, D.; Mays, L. *Applied Hydrology*; McGraw-Hill, 1988;
51. Koutsoyiannis, D.; Xanthopoulos, T. *Engineering Hydrology*; 3rd ed.; National Technical University of Athens: Athens, 1999;
52. Efstratiadis, A.; Koussis, A.D.; Koutsoyiannis, D.; Mamassis, N. Flood design recipes vs. reality: Can predictions for ungauged basins be trusted? *Nat. Hazards Earth Syst. Sci.* **2014**, *14*, 1417–1428, doi:10.5194/nhess-14-1417-2014.
53. Mockus, V.; McKeever, V.; Owen, W.; Rallison, R. Design Hydrographs. In *NATIONAL ENGINEERING HANDBOOK*; United States Department of Agriculture - Natural Resources Conservation Service, 1972.
54. Michailidi, E.M.; Antoniadi, S.; Koukouvinos, A.; Bacchi, B.; Efstratiadis, A. Timing the time of concentration: shedding light on a paradox. *Hydrol. Sci. J.* **2018**, *63*, 721–740, doi:10.1080/02626667.2018.1450985.
55. Feldman, A.D. *Hydrologic Modeling System Technical Reference Manual*; 2000;
56. Dottori, F.; Di Baldassarre, G.; Todini, E. Detailed data is welcome, but with a pinch of salt: Accuracy, precision, and uncertainty in flood inundation modeling. *Water Resour. Res.* **2013**, *49*, 6079–6085, doi:10.1002/wrcr.20406.
57. Brunner, G.W. HEC-RAS River Analysis System - Hydraulic Reference Manual, Version 5.0. US Army Corps of Engineers–Hydrologic Engineering Center 2016, 547.
58. Paz, A.R. da; Collischonn, W.; Tucci, C.E.M.; Padovani, C.R. Large-scale modelling of channel flow and floodplain inundation dynamics and its application to the Pantanal (Brazil). *Hydrol. Process.* **2011**, *25*, 1498–1516, doi:10.1002/hyp.7926.
59. Tsubaki, R.; Fujita, I. Unstructured grid generation using LiDAR data for urban flood inundation modelling. *Hydrol. Process.* **2010**, *24*, 1404–1420, doi:10.1002/hyp.7608.
60. Teng, J.; Vaze, J.; Dutta, D.; Marvanek, S. Rapid Inundation Modelling in Large Floodplains Using LiDAR DEM. *Water Resour. Manag.* **2015**, *29*, 2619–2636, doi:10.1007/s11269-015-0960-8.
61. Leitão, J.P.; de Sousa, L.M. Towards the optimal fusion of high-resolution Digital Elevation Models for detailed urban flood assessment. *J. Hydrol.* **2018**, *561*, 651–661, doi:10.1016/j.jhydrol.2018.04.043.
62. Bhuyian, M.N.M.; Kalyanapu, A. Accounting digital elevation uncertainty for flood consequence assessment. *J. Flood Risk Manag.* **2018**, *11*, S1051–S1062, doi:10.1111/jfr3.12293.
63. Bates, P.D.; De Roo, A.P.J. A simple raster-based model for flood inundation simulation. *J. Hydrol.* **2000**, *236*, 54–77, doi:10.1016/S0022-1694(00)00278-X.
64. Bharath, R.; Elshorbagy, A. Flood mapping under uncertainty: a case study in the Canadian prairies. *Nat. Hazards* **2018**, *94*, 537–560, doi:10.1007/s11069-018-3401-1.
65. Liu, Z.; Merwade, V. Accounting for model structure, parameter and input forcing uncertainty in flood inundation modeling using Bayesian model averaging. *J. Hydrol.* **2018**, *565*, 138–149, doi:10.1016/j.jhydrol.2018.08.009.
66. Liu, Z.; Merwade, V.; Jafarzadegan, K. Investigating the role of model structure and surface roughness in generating flood inundation extents using one- and two-dimensional hydraulic models. *J. Flood Risk Manag.* **2019**, *12*, doi:10.1111/jfr3.12347.
67. Brown, J.D.; Spencer, T.; Moeller, I. Modeling storm surge flooding of an urban area with particular reference to modeling uncertainties: A case study of Canvey Island, United Kingdom. *Water Resour. Res.* **2007**, *43*, 1–22, doi:10.1029/2005WR004597.
68. Schubert, J.E.; Sanders, B.F. Building treatments for urban flood inundation models and implications for predictive skill and modeling efficiency. *Adv. Water Resour.* **2012**, *41*, 49–64, doi:10.1016/j.advwatres.2012.02.012.
69. Bellos, V.; Tsakiris, G. Comparing Various Methods of Building Representation for 2D Flood Modelling In Built-Up Areas. *Water Resour. Manag.* **2015**, *29*, 379–397, doi:10.1007/s11269-014-0702-3.
70. Shen, J.; Tan, F.; Zhang, Y. Improved building treatment approach for urban inundation modeling: A case study in Wuhan, China. *Water (Switzerland)* **2018**, *10*, 1–24, doi:10.3390/w10121760.

71. Teng, J.; Jakeman, A.J.; Vaze, J.; Croke, B.F.W.; Dutta, D.; Kim, S. Flood inundation modelling: A review of methods, recent advances and uncertainty analysis. *Environ. Model. Softw.* **2017**, *90*, 201–216, doi:10.1016/j.envsoft.2017.01.006.
72. Special Secretariat for Water; Ministry of Environment and Energy (SSW-MEE). *Preliminary Flood Risk Assessments*; 2013;
73. European Commission *European Overview - Flood Risk Management Plans Accompanying*; 2019;
74. US Army Corps of Engineers - Hydrologic Engineering Center HEC-HMS Technical Reference ManualChannel - FlowCurrent - Muskingum Model Available online: https://www.hec.usace.army.mil/confluence/hmsdocs/hmstrm/channel-flow/musk-ingum-model (accessed on Mar 2, 2021).
75. Brunner, G.W.; CEIWR-HEC HEC-RAS River Analysis System 2D Modeling User ' s Manual. US Army Corps of Engineers – Hydrologic Engineering Center. 2016.
76. Brunner, G.W.; CEIWR-HEC HEC-RAS River Analysis System 2D Modeling User ' s Manual. US Army Corps of Engineers – Hydrologic Engineering Center. 2016.
77. European Environment Agency *Disasters in Europe: more frequent and causing more damage*; 2011;
78. Papaioannou, G. Flood Hazard and Risk Modelling Framework for Ungauged Streams and Watersheds, University of Thessaly, 2017.
79. Alamanos, A.; Latinopoulos, D.; Loukas, A.; Mylopoulos, N. Comparing Two Hydro-Economic Approaches for Multi-Objective Agricultural Water Resources Planning. *Water Resour. Manag.* **2020**, *34*, 4511–4526, doi:10.1007/s11269-020-02690-6.
80. Fletcher, S.; Strzepek, K.; Alsaati, A.; De Weck, O. Learning and flexibility for water supply infrastructure planning under groundwater resource uncertainty. *Environ. Res. Lett.* **2019**, *14*, doi:10.1088/1748-9326/ab4664.
81. Islam, Z. Literature Review on PHYSICALLY BASED HYDROLOGIC MODELING, University of Alberta, 2011.